AD-A178 282 ATOMISIIC STUDY OF METASTABLE PHASES IN AN Al-3WT%-Li0 1/1
12WT%-ZR ALLOY A P..(U) PENNSYLVANIA UNIV PHILADELPHIA
DEPT OF MATERIALS SCIENCE AND E.. H W PICKERING
UNCLASSIFIED 02 MAR 87 N00014-84-K-0201 F/G 11/6 NL

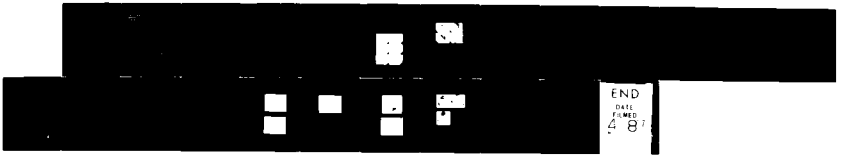

END
DATE FILMED
4 87

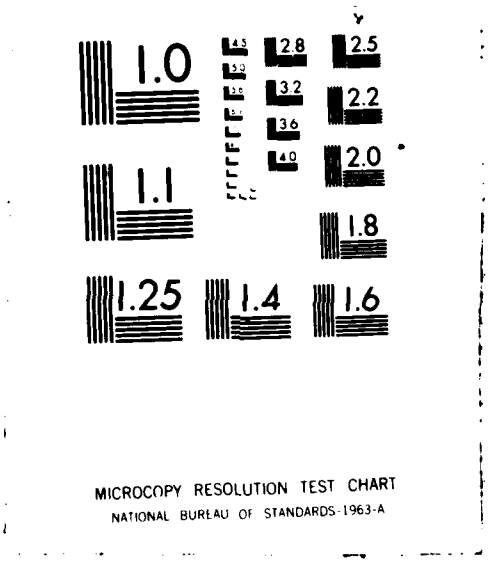
1.0
1.1
1.25
1.4
1.6
1.8
2.0
2.2
2.5
2.8
3.2
3.6
4.0
MICROCOPY RESOLUTION TEST CHART
NATIONAL BUREAU OF STANDARDS-1963-A

COLLEGE OF EARTH AND MINERAL SCIENCES

DEPARTMENT OF MATERIALS SCIENCE

METALLURGY PROGRAM

TECHNICAL REPORT

March 2, 1987

OFFICE OF NAVAL RESEARCH

Contract No. N00014-84-k-0201

1. ATOMISTIC STUDY OF METASTABLE PHASES IN AN Al-3wt.%-Li-0.12wt.%-Zr ALLOY

2. A PRELIMINARY STUDY OF Al-Li ALLOYS USING ATOM-PROBE FIELD ION MICROSCOPY AND TRANSMISSION ELECTRON MICROSCOPY

Howard W. Pickering

Department of Materials Science & Engineering
The Pennsylvania State University

The Pennsylvania State University

University Park, Pennsylvania

THE PENNSYLVANIA STATE UNIVERSITY

College of Earth and Mineral Sciences

UNDERGRADUATE PROGRAMS OF STUDY

Ceramic Science and Engineering, Earth Sciences, Fuel Science, Geography, Geosciences, Metallurgy, Meteorology, Mineral Economics, Mining Engineering, Petroleum and Natural Gas Engineering, and Polymer Science.

GRADUATE PROGRAMS AND FIELDS OF RESEARCH

Ceramic Science, Fuel Science, Geochemistry and Mineralogy, Geography, Geology, Geophysics, Metallurgy, Meteorology, Mineral Economics, Mineral Processing, Mining Engineering, Petroleum and Natural Gas Engineering, and Polymer Science.

UNIVERSITY-WIDE INTERDISCIPLINARY GRADUATE PROGRAMS INVOLVING E&MS FACULTY AND STUDENTS

Earth Sciences, Ecology, Environmental Pollution Control Engineering, Mineral Engineering Management, Operations Research, Regional Planning, and Solid State Science.

ASSOCIATE DEGREE PROGRAMS

Metallurgical Engineering Technology and Mining Technology.

INTERDISCIPLINARY RESEARCH GROUPS WITHIN THE COLLEGE

Coal Research, Ore Deposits Research, Earth System Science, and the Mining and Mineral Resources Research Institute.

ANALYTICAL AND STRUCTURAL STUDIES

Classical chemical analysis of metals and silicate and carbonate rocks; X-ray crystallography; electron microscopy and diffraction; electron microprobe analysis; atomic absorption analysis; spectrochemical analysis; surface analysis by secondary ion mass spectrometry (SIMS); and scanning electron microscopy (SEM).

U.Ed. 9-725

SECURITY CLASSIFICATION OF THIS PAGE (When Data Entered)

REPORT DOCUMENTATION PAGE

READ INSTRUCTIONS BEFORE COMPLETING FORM

1. REPORT NUMBER: Technical Report, March 2, 1987	2. GOVT ACCESSION NO.
3. RECIPIENT'S CATALOG NUMBER	
4. TITLE (and Subtitle): Atomistic Study of Metastable Phases in an Al-3wt.%-Li-0.12wt.%-Zr Alloy & A Preliminary Study of Al-Li Alloys Using Atom-Probe Field Ion Microscopy and Transmission Electron Microscopy	5. TYPE OF REPORT & PERIOD COVERED: Technical Report
	6. PERFORMING ORG. REPORT NUMBER
7. AUTHOR(s): H. W. Pickering	8. CONTRACT OR GRANT NUMBER(s): N00014-84-k-0201
9. PERFORMING ORGANIZATION NAME AND ADDRESS: Metallurgy Program, 209 Steidle Building, The Pennsylvania State University, University Park, PA 16802	10. PROGRAM ELEMENT, PROJECT, TASK AREA & WORK UNIT NUMBERS
11. CONTROLLING OFFICE NAME AND ADDRESS	12. REPORT DATE: March 2, 1987
	13. NUMBER OF PAGES
14. MONITORING AGENCY NAME & ADDRESS (if different from Controlling Office)	15. SECURITY CLASS. (of this report)
	15a. DECLASSIFICATION/DOWNGRADING SCHEDULE

16. DISTRIBUTION STATEMENT (of this Report)

17. DISTRIBUTION STATEMENT (of the abstract entered in Block 20, if different from Report)

18. SUPPLEMENTARY NOTES

19. KEY WORDS (Continue on reverse side if necessary and identify by block number)

20. ABSTRACT (Continue on reverse side if necessary and identify by block number)

Two aluminum-lithium alloys, one containing 2 wt% Li and the other 3wt%Li-0.12wt%Zr, have been examined using transmission electron microscopy (TEM), field-ion microscopy (FIM) and atom-probe field-ion microscopy (APFIM). The results show that both FIM and APFIM are potentially the most powerful techniques for the analysis of Li-containing alloys, because Li can be detected and analyzed quantitatively using the APFIM. Good correlation between the FIM images of the δ' (Al_3Li) and the β' (Al_3Zr), with those obtained using conventional TEM imaging has been obtained.

Finally, β' in the aged Al-Li-Zr alloy has been shown to be virtually stoichiometric and Li incorporation in the β' is suggested to be a minor effect

DD FORM 1 JAN 73 1473 EDITION OF 1 NOV 65 IS OBSOLETE
S/N 0102-LF-014-6601

SECURITY CLASSIFICATION OF THIS PAGE (When Data Entered)

Scripta METALLURGICA Vol. 20, pp. 1131-1136, 1986 Pergamon Journals Ltd.
Printed in the U.S.A.

Atomistic Study of Metastable Phases in an Al-3wt.%-Li-0.12wt.%-Zr Alloy

Toshio Sakurai, A. Kobayashi, Y. Hasegawa, A. Sakai and H. W. Pickering*

The Institute for Solid State Physics (ISSP), The University of Tokyo
Minato-ku, Tokyo, JAPAN

* Department of Materials Science & Engineering
The Pennsylvania State University, University Park, PA 16802 USA

(Received April 29, 1986)
(Revised May 27, 1986)

Introduction

The Al-Li based alloy system has been intensively studied recently because of its importance as a light-weight aerospace material.(1-3) The addition of every weight percent of lithium in the Al matrix reduces the density of Al alloys by 3.5% up to the solubility limit and increases their strength and elastic modulus.(4) Corrosion resistance and fatigue characteristics are also improved by means of ultrafine grain size and solute hardening.(5) These beneficial effects, however, are accompanied by a reduction in ductility and toughness to unacceptably low levels for structural applications.(6) This is attributed to the shearable nature of the coherent f.c.c. $L1_2$-type metastable δ' phase, formed during ageing and even during the quench, invariably, from the solution treatment temperature.(6,7)

Various third elements are usually added for the purpose of increasing the δ'/β' misfit to suppress these detrimental side effects.(8-10) In spite of the significant effort devoted to understanding the behaviour of lithium and third elements in Al-Li based alloys, their exact roles in the alloys are still unknown, mainly because most conventional analytical techniques experience great difficulty in detecting and quantifying lithium on an atomic scale.(11)

The addition of zirconium among other elements (Mg, Zn, Ag, etc) is known to improve toughness and stress corrosion resistance in the temperature range between 100 and 200°C by suppressing recrystallization.(12-14) It has been reported that Al-Li-Zr alloys are partially recrystalilized and have fine subgrains of 1-2 μm in diameter and a small volume fraction of Al_3Zr dispersoids (β' phase) in the Al-Li matrix.(14) Some researchers have recently suggested on the basis of X-ray diffraction studies that the so-called β' phase contains a significant amount of Li.(12,13) The precise information on the microstructures of the β' and δ' phases is most valuable in order to understand the recrystallization processes.

High-performance time-of-flight atom-probe field ion microscopy (ToF atom-probe (FIM)) is a powerful technique for the study of the structures and chemical compositions of the initial-stage precipitates in the Al-Li based alloys, since it is capable of observing atomic arrangements of a small region on truly an atomic scale and simultaneously analyzing each individual atom as to its chemical identity.(15,16) We report in this paper the first successful, quantitative investigation of the metastable phases, β' and δ' in the Al-3wt.%Li- 0.12wt.%Zr alloy using the FIM and ToF atom-probe.

FIM Observation

The Al-Li-Zr alloy specimen was solution treated by annealing at 550°C for 1 h and water quenched. Four different ageing conditions studied were 150°C for 30 min or 3,000 min, and 200°C for 30 min or 1,000 min. The specimen was

0036-9748/86 $3.00 + .00

electro-chemically polished into a sharp needle of approximately 100 nm radius.(17) Field ion (FI) imaging was performed on a 125 mm diameter curved chevron channelplate optical-fibre screen assembly at the specimen temperature of 20 K using either pure Ne gas or a Ne-H_2 gas mixture. It was found to be rather difficult to obtain stable and detailed FI images exihibiting all three regions, Zr-rich β', Li-rich δ', and the Al matrix, since the specific evaporation fields differ so much among them (3.5, 1.1 and 2.1 V/A, for Zr, Li and Al, respectively). Nevertheless, good quality FI images were obtained detailing the structures of the α Al matrix, δ' phase and the so-called β' phase.

Fig. 1 (A-F) is a series of FI micrographs taken during field evaporation of the specimen aged at 200°C for 1,000 min showing the evolution of two β' phase precipitates (marked as I) enveloped by the thick δ' phase (II). While the β' precipitate at the lower left corner becomes smaller and smaller as the surface layers gradually evaporate (A to C), a small β' precipitate emerges at three o'clock (C and D). Both β' precipitates disappear after evaporating approximately 75 layers of the (111) plane, leaving the large δ' phase precipitates (D to F). The δ' precipitate is somewhat difficult to distinguish from the Al matrix (indicated by arrows in B, C, and E), but a slight change in the imaging condition (reducing the surface electric field and increasing H_2 gas pressure) helps visualizing the δ' phase and its sharp boundary with the Al matrix.

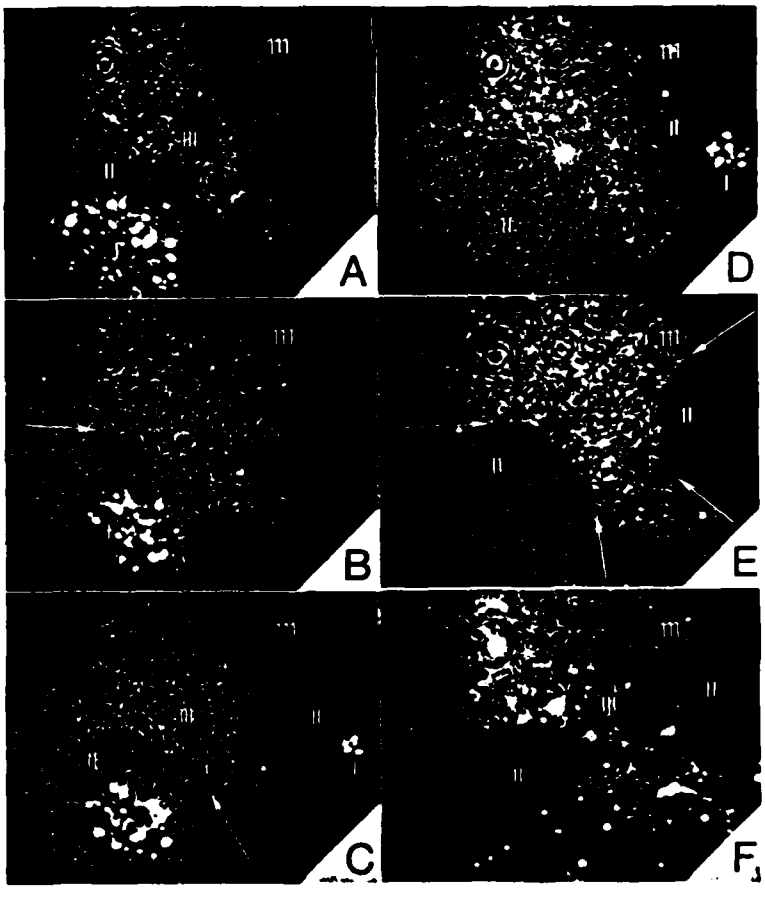

Fig. 1. A series of FI micrographs taken during gradual layer-by-layer field evaporation of the Al-3wt.%Li-0.12wt.% Zr alloy aged at 200°C for 1,000 min. The evolution of two bright β' precipitates (I) with the Li-rich dark δ' envelope (II) is shown (lines indicate positions of the phases boundaries).

Fig. 2 is a similar sequence of the FI micrographs of the alloy specimen with the same ageing condition as in Fig. 1 but shows the evolution of one precipitate surrounded by the δ' phase and two δ' precipitates. By continuously evaporating the Al matrix (A), the δ' precipitate emerged at 9 o'clock (B). Further evaporation of the surface region resulted in emergence of two additional precipitates: one is a composite β' precipitate enveloped by δ' phase at 6 o'clock and two other δ' precipitates at 4 and 10 o'clock (C and D).

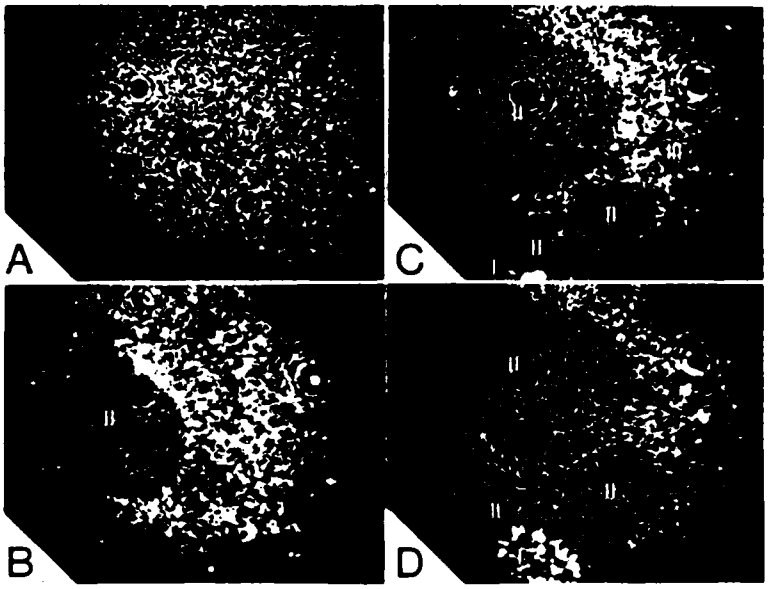

Fig. 2. A series of FI micrographs showing the evolution of one β' precipitate (I) and two dark δ' precipitates (II) in the alloy aged at 200°C for 1,000 min. Coherency between the δ' precipitate (II) and the α Al matrix (III) is evident.

The β' phase is imaged brightly and the δ' phase is usually imaged dark. Both of them, however, are imaged sparsely, compared with the Al matrix. The β' precipitate is easily recognized because it is much brighter than the Al matrix and only Zr is imaged. The δ' precipitate is almost completely coherent with the Al matrix as is evident in Figs. 1 D and E and Figs. 2 B and D, and only Al is imaged in the δ' precipitate. Therefore, their interface usually is difficult to recognize (Figs. 1 A to D and Fig. 2 D).

The composite precipitate of the β' phase enveloped by the δ' phase was observed only in the specimens annealed at 200°C for 1,000 min. In all other specimens, β' and δ' appeared as separate precipitates distributed randomly. This is contrary to some TEM observations that the β' precipitate was enveloped by the δ' phase already upon ageing at 150°C for 30 min.(17) The sizes of the β' and δ' precipitates vary widely in a range of 5 and 50 nm in diameter, even within an individual specimen. The larger δ' envelopes had a diameter well over 100 nm. It was noted that the β' precipitate often was not located at the center of the larger δ' precipitate. There is some indication that the dependence of the size on the ageing temperature of the β' precipitate is insignificant. This observation, however, could be atypical, i.e., a product of the small quantity of precipitates studied.(3,18)

Atom-Probe Analysis

In order to obtain compositional information on the β' and δ' precipitates and the Al matrix, the ToF atom-probe analysis was performed by setting the probe-hole wholly within region I of Fig. 1 A. The results are

shown in Fig. 3, where the cumulative numbers of Zr and Li atoms are plotted against the cumulative number of total signals (Al + Li + Zr). Since there were approximately 70 atoms/layer within the probe-hole, as estimated from examination of the data for successive layer-by-layer evaporation, the data in Fig. 3 are for a depth of approximately 250 atomic layers. The three diffrent regions of Fig. 3 are identified as follows: the initial Zr-rich region (I) is the β' precipitate, the next Li-rich region (II) is the δ' phase which envelops the β' phase, and the last Al-rich region (III) is the α Al matrix.

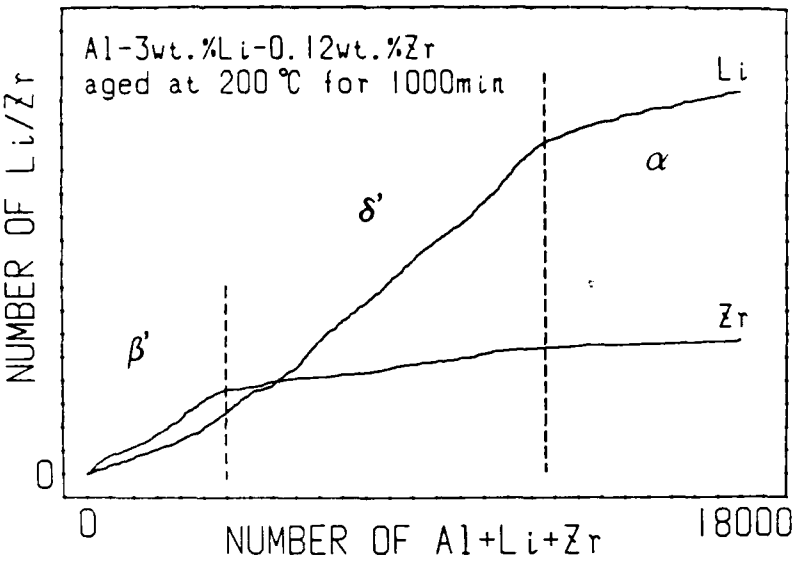

Fig. 3. Atom-probe compositional depth profile of the region encompassing the bright β' precipitate, the dark δ' envelope, and the Al matrix in the alloy aged at 200°C for 1,000 min, shown in Fig. 1.

Fig. 4 presents similar atom-probe data for a sample in the as-quenched state obtained by analyzing the interface region of the precipitate and Al matrix region. The initial Zr-rich region is the bright β' precipitate and the following region is the Li saturated Al matrix.

It is not yet possible to determine the chemical compositions of various metastable phases found in the Al-Li-Zr alloys on an absolute scale, since the evaporation behaviours of the three elements are so different. It was found that the conventional procedure of using a large pulse fraction did not work for equal detection sensitivity of the three elements. Therefore, the following two assumptions were made in the present atom-probe analysis: (a) the Li concentration in the supersaturated solid solution in the as-quenched state was the nominal 3 wt.% (11.0 at.%), and (b) the Li concentration in the δ' precipitates formed by ageing was 25 at.%, based on the well-established $L1_2$ type Al_3Li structure. With these assumptions, the chemical compositions were determined and are listed below.

condition	" β' " phase	δ' phase	α matrix
as-quench	Zr:15 -22at.%	Zr: <.1at.%	Zr: 0 at.%
	Li: 5 -11at.%	Li: ≈20at.%	Li: (11at.%)
150°C	Zr:18 -23at.%	Zr: <.1at.%	Zr: <.1at.%
for 1,000 min	Li: 3 - 5at.%	Li: (25at.%)	Li: 2-7at.%
200°C	Zr:22 -27at.%	Zr: <.1at.%	Zr: <.1at.%
for 30 min	Li: 1 - 5at.%	Li: (25at.%)	Li: 3-7at.%
200°C	Zr:20 -27at.%	Zr: <.1at.%	Zr: <.1at.%
for 1,000min	Li: 2 - 7at.%	Li: (25at.%)	Li: 3-6at.%

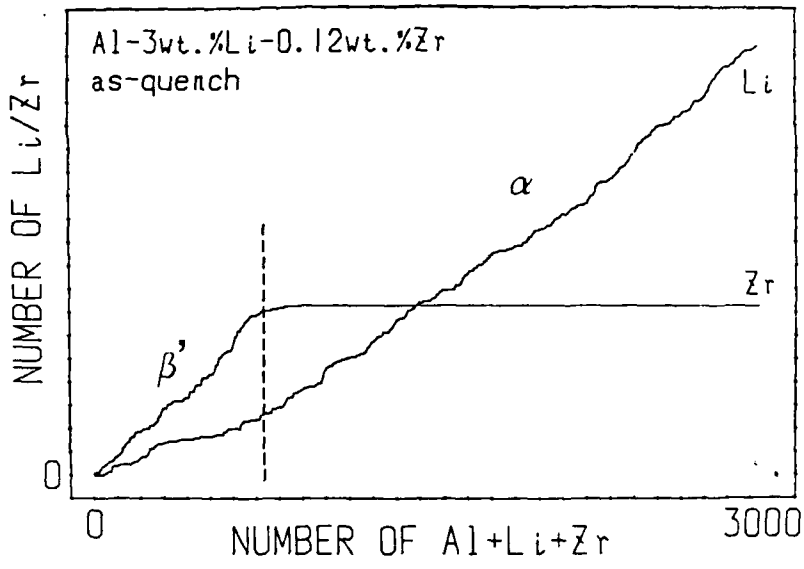

Fig. 4. Atom-probe depth profile of the interface region of the bright β' precipitate and the supersaturated Al-Li matrix for the as-quenched state.

Discussion and Summary

The conclusions based on the above FIM and atom-probe analyses of the Al-3wt.%Li-0.12wt.%Zr alloy are as follows:
(1) Both the β' and δ' phases can be clearly imaged realizing atomic scale details by field ion microscopy.
(2) The darkly imaged δ' precipitate is coherent with the Al matrix, while the bright β' precipitate does not appear to be coherent on the basis of FIM observations with both the δ' phase and the Al matrix.
(3) The so-called β' precipitates contain significant levels of Li: 5 to 11 at.% in the as-quenched state and 1 to 7 at.% as a result of ageing at 200 °C, while the Zr level varies in a range of 15 to 27 at.%.
(4) The Li concentration in the α Al matrix is 2 to 7 at.% and 3 to 7 at.% after ageing at 150 and 200 °C, respectively.

The FIM observations of the β' and δ' precipitates in the present paper generally agree well with TEM observations(12,17) as to their size and distribution as well as their coherency with the Al matrix.

There have been conflicting reports as to the chemical composition of the β' precipitate.(12,13) However, the data in the present work clearly suggest that the partitioning of Li is significant in the β' precipitate, particularly in the case of the as-quenched state. The Li concentration in the as-quenched case is almost as high as that in the supersaturated solid solution. As the ageing proceeds, the Li concentration decreases (Table); the lowest level observed so far is 2.5 at.%. This result, however, does not agree with a recent report based on TEM and energy loss spectroscopy analyses that the Li level may be as high as 45 to 80 at.%.(13) Other interesting observations are that the composition changes abruptly (atomic scale) at the interfaces between the β' phase and the δ' phase or the Al matrix, and that the Zr and Li concentrations appear to be uniform within the precipitates regardless of their shape and/or size.

In conclusion, FIM and ToF atom-probe investigations have successfully been carried out on the metastable phases, the so-called β' and δ' precipitates, in the Al-3wt.%Li-0.12wt.%Zr alloy under various heat

treatments. Taking advantages of the ToF atom-probe, that is capable of detecting all elements including light elements, the Li concentrations were determined in the β' phase and the α Al matrix.

Acknowledgements

We would like to thank T. Abe, K. Hono and N. Sano for technical assistance and fruitful discussions. The Al alloy was kindly supplied by Alcoa Technical Center. This work was partially supported by the Office of Naval Research, Contract No. N00014-84-k-0201.

References

1. J. M. Silcock, J. Inst. Metals, 88, 357 (1959/60). and T. Yoshiyama, and K. Hasebe, J. Phys. Soc. Japan, 25, 908 (1968).
2. M. Tamura, T. Mori and T. Nakamura, J. Jpn. Inst. Met. 34, 919 (1970).
3. B. E. Noble and G. E. Thompson, Metal Sci. J. 5, 114 (1971).
4. B. Noble, S. J. Harris and K. Dinsdale, J. Mater. Sci. 17, 461 (1982)
5. P. Niskanen, T. H. Sanders Jr., M. Marek and J. G. Rinker, Aluminum-Lithium Alloys (eds. T. H. Sanders Jr. and E. A. Starke Jr.) p. 347 TMS-AIME (1981).
6. T. H. Starke Jr. and E. A. Starke Jr., Acta Met. 30, 927 (1982).
7. T. H. Sanders Jr., Aluminum-Lithium Alloys (eds. T. H. Sanders Jr. and E. A. Starke Jr.) p. 63 TMS-AIME (1981).
8. F. W. Gayle, Aluminum-Lithium Alloys (eds. T. H. Sanders Jr. and E. A. Starke Jr.) p. 119 TMS-AIME (1981).
9. P. J. Gregson and H. M. Flower, Acta Metall. 33, 527 (1985).
10. W. A. Cassada, G. J. Shiflet and E. A. Starke Jr., Acta Metall. 34, 367 (1986).
11. D. B. Williams and P. R. Howell, to be submitted.
12. F. W. Gayle and J. B. Vander Sande, Scripta Metall. 18, 473 (1984).
13. F. W. Gayle and J. B. Vander Sande, Proc. ASTM Conf. on Rapidly Solidified Powder Aluminum Alloys, p. (1984).
14. S. M. L. Sastry and J. E. O'Neal, Aluminum-Lithium Alloys II (eds. T. H. Sanders Jr. and E. A. Strake Jr.) p. 79 TMS-AIME (1984).
15. T. Sakurai, T. Hashizume and A. Jimbo, Appl. Phys. Lett. 44, 38 (1984).
16. K. Hono, T. Hashizume, Y. Hasegawa, K. Hirano and T. Sakurai, Scripta Metall. 20, 487 (1986).
17. K. Hono, T. Abe, H. W. Pickering, P. R. Howell, Y. Hasegawa, T. Sakurai, N. Sano and K. Hirano, Proc. of Intern. Conf. on Aluminum Alloys, (1986).
18. J. H. Kulwicki and T. H. Sanders Jr., Aluminum-Lithium Alloys (eds. T. H. Sanders Jr. and E. A. Starke Jr.) p. 63 TMS-AIME (1981).

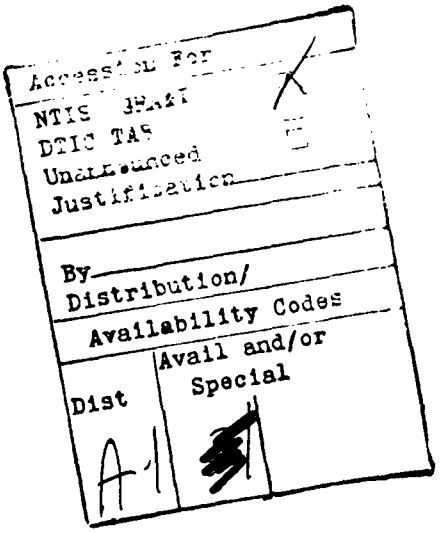

ALUMINUM ALLOYS – PHYSICAL AND MECHANICAL PROPERTIES
E. A. Starke, Jr and T. H. Sanders, Jr. Editors. Engineering Materials Advisory Services LTD, Warley, West Midlands U.K. 1986.

A PRELIMINARY STUDY OF Al-Li ALLOYS USING ATOM-PROBE FIELD ION MICROSCOPY AND TRANSMISSION ELECTRON MICROSCOPY

K. Hōno, T. Abe, D.R. Hess, H.W. Pickering, and P.R. Howell*
Y. Hasegawa and T. Sakurai**
N. Sano and K. Hirano***

Two aluminum-lithium alloys, one containing 2 wt% Li and the other 3wt%Li-0.12wt%Zr, have been examined using transmission electron microscopy (TEM), field-ion microscopy (FIM) and atom-probe field-ion microscopy (APFIM). The results show that both FIM and APFIM are potentially the most powerful techniques for the analysis of Li-containing alloys, because Li can be detected and analyzed quantitatively using the APFIM. Good correlation between the FIM images of the δ' (Al_3Li) and the β' (Al_3Zr), with those obtained using conventional TEM imaging has been obtained.

Finally, β' in the aged Al-Li-Zr alloy has been shown to be virtually stoichiometric and Li incorporation in the β' is suggested to be a minor effect.

INTRODUCTION

As noted by Williams and Howell (1), one of the major stumbling blocks to the quantitative analysis of Li-containing Al alloys is the inability of most techniques to detect Li, and to analyze Li quantitatively, on a scale which is of the greatest importance (i.e. less than approximately 50 nm). Although electron energy loss spectroscopy (EELS) can detect Li, the detectability limit for Li using EELS is probably of the order of at least several atomic % (Chan and Williams (2)). The APFIM is unique in many respects since it can detect all elements with equal efficiencies and therefore has the capabilities to answer certain questions that still remain concerning the nature of Al-Li-X alloys. However, since both the FIM and APFIM can only analyze very small volumes ($\sim 10^{-16} m^3$), the most convincing FIM/APFIM results are those

* Department of Materials Science and Engineering, The Pennsylvania State University, University Park, PA 16802, USA
** The Institute for Solid State Physics, The University of Tokyo, Roppongi, Tokyo, 106, Japan
*** Department of Materials Science, Tohoku University, Sendai, 980, Japan

which have employed TEM as a parallel investigative technique.

In this paper FIM, APFIM and TEM have been used to examine the microstructures of a binary Al-Li alloy and a ternary Al-Li-Zr alloy. It is shown that the FIM can image both δ' (Al_3Li) and β' (Al_3Zr) and that a good correlation exists between the FIM/APFIM and the TEM results. The β' phase has been analyzed quantitatively using the APFIM data. In view of the fact that this is only a preliminary study, a discussion of certain problems which may be resolved by the APFIM, precedes the results which have been obtained to date.

Some Unanswered Questions

At present, there is no universally accepted Al-Li phase diagram. For example, Gayle and Vander Sande (3) have proposed that the two phase α + δ' phase field is associated with a monotectoid reaction, whereas Sigli and Sanchez (4) have calculated a phase diagram in which the δ' is more stoichiometric than the Gayle and Vander Sande proposal. In addition, the monotectoid is not present in the calculated diagram of Sigli and Snachez. The existence of a miscibility gap (α + α') within the α + δ' phase field has also been suggested (4), and indirect evidence for this miscibility gap has been obtained by Nozato and Nakai (5), Spooner et al.(6), Rioja and Ludwiczak (7), Papzian et al.(8). However, direct imaging of the α + α' structure has not proved possible.

A number of Li and Cu containing transition phase (eg., T'_1, T'_2, T'_B) have been suggested to form in ternary Al-Li-Cu alloys (7). However, as noted by Sainfort and Guyot (9) it is unlikely that TEM based techniques will be able to analyze the composition of these, and other phases.

There is a continuing controversy concerning the reason why the β' phase images as a dark imaging "core" in superlattice dark fields of duplex δ'/β' precipitates. Gayle and Vander Sande (10) proposed that Li incorporation into the Zr sub-lattice of the β' could lead to a zero intensity in eg., a 100 centered dark field (CDF) image. These authors calculated the structure factor for g=100 ($F_{g=100}$) as a function of the Li content of the β' and showed that for a composition of $Al_3(Li_{0.58}Zr_{0.42})$, $F_{g=100}$ would be zero. Thus the present investigation aims to document the composition of the β' and to check the validity of the explanation for the dark imaging core proposed by Gayle and Vander Sande.

EXPERIMENTAL

Two alloys were supplied by the Alloy Technology Division of Alcoa Laboratories Alcoa Center PA and had the following nominal compositions (wt%):

Al-2%Li

Al-3%Li-0.12%Zr.

Specimens for FIM and APFIM were prepared from ingots by swaging and drawing to 0.4 mm diameter wires. The wires were solution treated at 550°C for 15 min. under He and iced-water quenched. Aging was performed at either 150°C or 200°C. The samples were electropolished using a solution of 95% HNO_3 with 5% H_2O at 3V a.c.

Field-ion images were obtained at a specimen temperature of 20 to 30 K using Ne, He or their mixture at a pressure of $5x10^{-5}$ Torr as the imaging gas. APFIM analyses were performed in vacuum (10^{-11} Torr) using an energy compensated time-of-flight atom-probe.

Specimens for TEM were prepared from the same ingots but were hot-rolled prior to solution treating and aging. Thin foils were prepared in a twin-jet electropolisher using 25% nitric acid in methanol and an applied potential of 12 V. All TEM was performed on a Philips EM420T.

RESULTS

Fig. 1 is a β' CDF from the solution treated and quenched Al-3%Li-0.12%Zr alloy. Most of the β' precipitates are brightly imaging which suggests that if Li is substituting for Zr in the β', the extent of this substitution is relatively small*.

Fig. 2 is from the Zr containing alloy which had been aged for 1000 min at 150°C. In addition to the small spherical δ', duplex δ'/β' precipitates are observed. These duplex precipitates have been documented previously by eg. Gayle and Vander Sande (10), Makin and Ralph (11), Tosten et al.(12), Stimson et al.(13). In common with previous investigations, the β' is only weakly imaged in the δ'/β' CDF.

Aging the Al-Li-Zr at 200°C for 30 min. leads to an increase in the β' size as evidenced by Fig. 3. In addition, the β' cores of the duplex δ'/β' precipitates (arrowed) exhibit near zero intensity in the superlattice CDF. A rather interesting observation with respect to Fig. 3 is that, in the majority of cases, the δ' coating is not continuous (eg. at A) but consists of discrete spherical caps. This should be compared with Fig. 1, where the δ' has fully enveloped the β'. Further mention of the discrete nature of the δ' on the β' at 200°C is deferred to the discussion section.

*It should be noted that the intensity in the 100 superlattice reflection is proportional to $(Fg=100)^2$.

FIM Observation of δ'

A field-ion image of the Al-2%Li alloy which had been aged at 150°C for 1000 min. is shown in Fig. 4a. This image was recorded using 10^{-5} Torr of a Ne/He mixture as the imaging gas and at a specimen temperature of 20 K. The δ' precipitates are the dark imaging regions in the α matrix and are approximately 5 to 10 nm in diameter. This correlates well with that determined using the TEM (Fig. 4b).

The image contrast of a precipitate in the FIM is usually determined by differences in the evaporation fields of the elemental species. For the present alloy, the evaporation field of Li is about 0.5 that of Al. Hence, surface Li atoms evaporate preferentially with respect to surface Al atoms, resulting in δ' precipitates whose surface curvature is much larger than the rest of the surface. The large surface curvature of the δ' then leads to the dark imaging characteristics of this phase.

The large difference in the evaporation fields for Al(3.0 V/A) and Li(1.6V/A) also leads to difficulties in obtaining fully quantitative chemical information concerning the δ'. Further work is in progress to obtain this quantitative data.

FIM and APFIM Studies on the β' Phase

Figures 5a-c are FIM images of a bright imaging phase and several prominent poles, for both this phase and the matrix, have been indexed on Fig. 5a,b. From Fig. 5 (and from other micrographs in this, and other evaporation sequences) it can be concluded that:

(i) the precipitate is ordered, i.e. the image exhibits a well-ordered structure;
(ii) the precipitate is cube/cube related to the α matrix;
(iii) the precipitates are spherical with diameters that are consistent with the size range of the β' as determined by TEM (≈20-50nm).

Hence, it can be concluded that the bright imaging precipitates are β'. The β' appear bright in the image due to the high evaporation field of Zr. FIM images of β' have also been obtained after aging at 200°C and the image characteristics are the same as those observed in the solution treated and quenched condition.

The composition of the β' in specimen material that had been aged for 30 min at 200°C, has been determined using APFIM. Fig. 6a is a cumulative plot of the number of Zr ions detected as a function of the total number of ions (Al+Li+Zr). Included on Fig. 6a is the predicted cumulative Zr plot for 25 at% Zr.

As can be seen, the β' is virtually stoichiometric. The position of the β' interface is arrowed on Fig. 6a and it can be seen that the level of Zr in the region adjacent to the precipitate is extremely low. It can also be noted from Fig. 6a that the β' interface is very sharp which is in agreement with the FIM images of Figs. 5a-c.

Fig. 6b is a plot of the absolute Zr concentration as a function of the number of ions detected (which is proportional to distance) for part of the data chain given in Fig. 6a. The observed fluctuation in concentration about the mean of 24.5 at% is due primarily to statistical counting errors (the total number of ions detected is only 600).

Fig. 6c is the cumulative plot of the number of Li signals as a function of the total number of ions detected. The Li concentration in the β' is appreciably constant at 2.4 at% and in common with the Zr distribution (Fig. 5a) there is a discrete change in the Li concentration at the β' interface.

DISCUSSION

The results of the present investigation have shown that the combination of FIM, APFIM and TEM is potentially a very powerful combination of analytical techniques for the study of Al-Li base alloys.

The results regarding the β' are particularly interesting in that reference to Figs. 6a,b shows that the Zr concentration is almost exactly 25 at%. This implies that the dark imaging cores of the duplex δ'/β' precipitates (Figs. 2, 3) as observed in the TEM are not caused by extensive incorporation of Li into the Zr sub-lattice of the β', since reference (10) suggested that the structure factor will be decreased only marginally by the substitution of 2.4 at% Li. This is also consistent with the observation that strong superlattice reflection from the β' are invariably observed in quenched specimen materials as shown both in this investigation and by other investigators (eg. Stimson et al. (13), Tosten and Howell (14), Galbraith and Howell (15)). However, this raises the question as to the explanation for the dark imaging characteristics of the β' when enveloped by δ'. Possible reasons include relative crystallographic rotations between the β' and δ' (13), and "imaging artifacts" due to the duplex nature of the δ'/β' precipitate.

Reference to Fig. 6c shows that the concentration of Li in the β' is higher than in the surrounding material, falling from 2.4 at% to less than 1 at%. This result was somewhat unexpected in that the β' is normally encapsulated by δ' which, according to the available phase diagrams should contain ≥25at%Li. However, at 200°C, the δ' coating is incomplete (Fig. 3). Hence, it is

likely that the probed interfacial region did not contain δ'. Due to the fact that the APFIM data are collected in vacuo, this hypothesis cannot be fully substantiated since the FIM image cannot be recorded during the APFIM analysis. However, preliminary semi-quantitative APFIM analyses of the δ' indicates the presence of a substantial Li content so it can be concluded tentatively that the region immediately adjacent to the β' precipitate which was analyzed, was most probably the α-matrix. Nonetheless, it should be noted that the Li concentration of <1 at% (Fig. 8c) is still well below the accepted solubility limit for Li in aluminum at 200°C. This may be explained by the fact that the pulse ratios used to analyze the β' were in the range of 0.2 to 0.3. For these pulse ratios, Li is evaporated preferentially from the α matrix and anomalously low Li concentrations are obtained. However, it should be appreciated that:

(i) at the imaging voltage, the β' image is completely stable and
(ii) for the pulse ratios employed (0.2 to 0.3) no preferential evaporation of the elemental species, Al and Zr, occurred.

Hence, from points (i) and (ii) and from the fact that the measured Al:Zr ratio is 3:1, it can be concluded that the Li content of the β' is not underestimated by any considerable extent and that the β' is virtually stoichiometric, i.e., its composition is close to Al_3Zr.

SUMMARY

Both δ' and β' have been imaged successfully using FIM and good correlation has been obtained between the FIM images and the corresponding TEM images. The composition of the β' has been documented using the APFIM and the results suggest that Li incorporation is at a low level. However, further work is required to obtain fully quantitative Li concentrations, both in the δ' and in the matrix.

REFERENCES

1. Williams, D. B. and Howell, P. R., in "Modern Aluminum Alloys" eds. Vasudevan, A. K. and Doherty, R. D., in press.
2. Chan, A. and Williams, D. B., Proceedings of the 3rd International Conference on Al-Li Alloys, The Institute of Metals, London, in press.
3. Gayle, F. W. and Vander Sande, J. B., Bull. Alloy Phase Diagrams, Vol. 5, 1984, p. 19.
4. Sigli, C. and Sanchez, J. M., Acta Met., in press.
5. Nozato, R. and Nakai, G., Trans. JIM, Vol. 18, 1977, p. 679.
6. Spooner, S., Williams, D. B. and Sung, C. M., Proceddings of the 3rd International Conference on Al-Li Alloys, The Institute of Metals, London, in press.

7. Rioja, R. J. and Ludwiczak, E. A., Proceedings of the 3rd International Conference on Al-Li Alloys, The Institute of Metals, London, in press.
8. Papazian, J. M., Sigli, C. and Sanchez, J. M., Scripta Met., in press.
9. Sainfort, P. and Guyut, P., Phil. Mag. A, Vol. 51, 1985, p. 575.
10. Gayle, F. W. and Vander Sande, J. B., Scripta Met., Vol. 18, 1984, p. 473.
11. Williams, D. B. and Edington, J. W., Met. Sci., Vol. 9, 1975, p. 529.
12. Makin, P. L. and Ralph, B. J., Mat. Sci., Vol. 19, 1984, p. 3835.
13. Tosten, M. H., Vasudevan, A. K. and Howell, P. R., Proceddings of the 3rd International Conference on Al-Li Alloys, The Institute of Metals, London, in press.
14. Stimson, W., Tosten, M. H., Howell, P. R., and Williams, D. B., Proceedings of the 3rd International Conference on Al-Li Alloys, The Institute of Metals, London, in press.
15. Tosten, M. H. and Howell, P. R., this Volume.
16. Galbraith, J. M. and Howell, P. R., this Volume.

ACKNOWLEDGEMENTS

Financial support for K. Hono and H. W. Pickering was provided by the Office of Naval Research, Contract No. N00014-84-K-0201. Financial support for P. R. Howell was provided by The Alloy Technology Division of Alcoa Laboratories, Alcoa Center, PA.

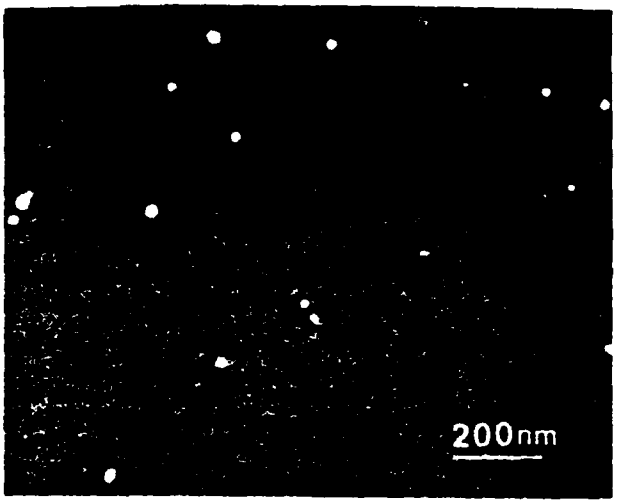

Fig. 1. Centered dark field image of the solution treated and quenched Al-3%Li-0.12%Zr.

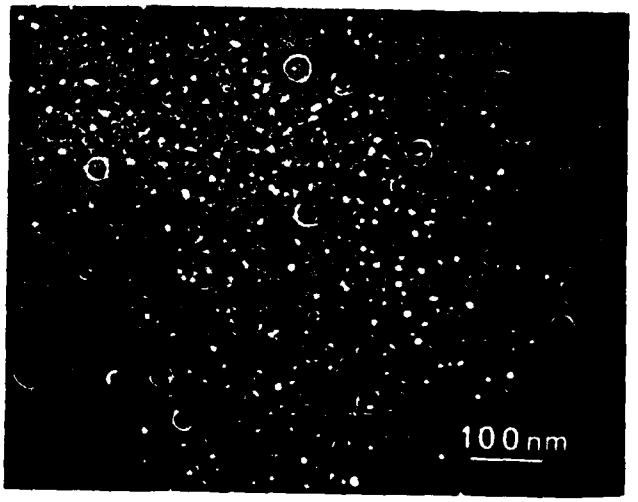

Fig. 2. Centered dark field image of Al-3%-0.12%Zr alloy aged at 150°C for 1000 min.

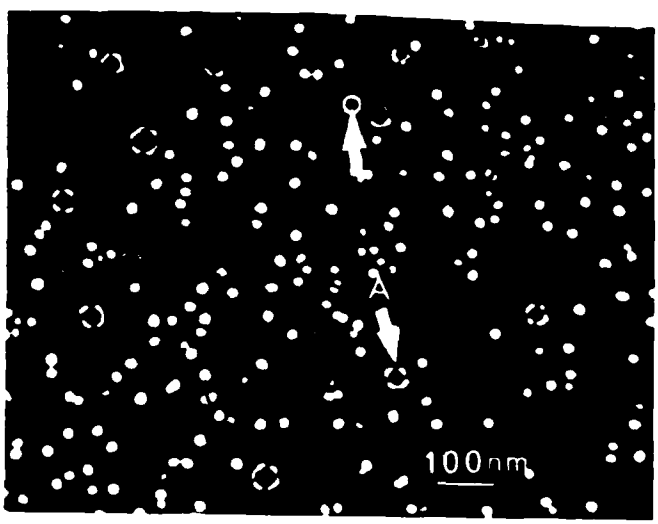

Fig. 3. Centered dark field image of Al-3%Li-0.12%Zr alloy aged at 200°C for 30 min.

Fig. 4a. A field-ion microscopic image of Al-2%Li aged at 150°C for 1000 min.

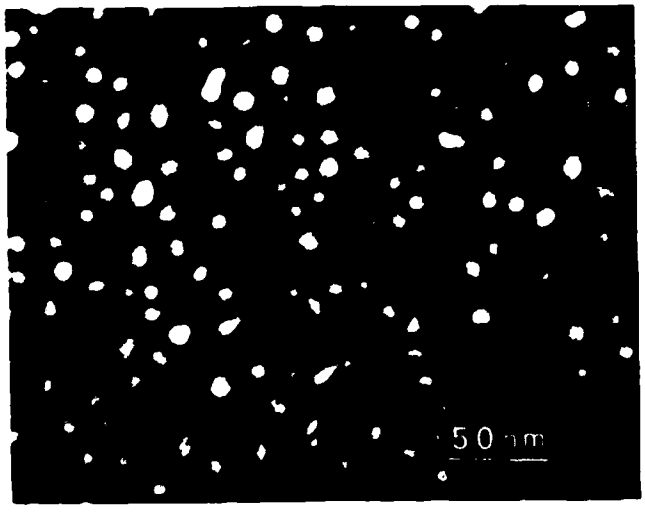

Fig. 4b. TEM image of Al-2%Li aged at 150°C for 1000 min.

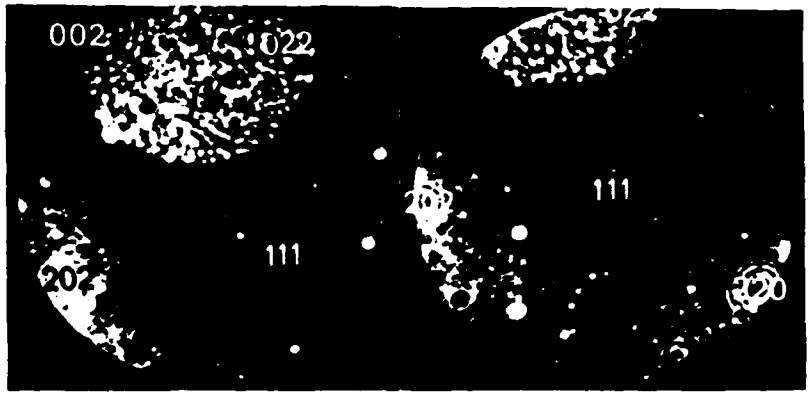

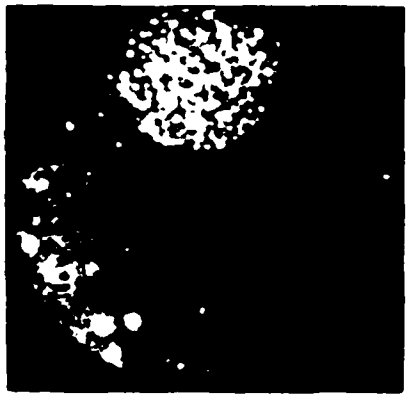

Fig. 5 Field-ion microscopic images of Al-3%Li-0.12%Zr alloy aged at 150°C for 1000 min. The bright imaging phase is '.

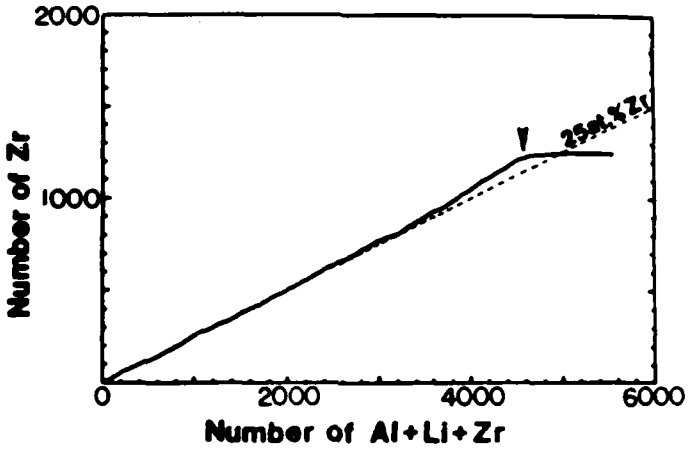

Fig. 6a. Cumulative number of Zr atoms detected as a function of tota total number of Al+Li+Zr for β' in Al-3%Li-0.12%Zr alloy aged at 200°C for 30 min.

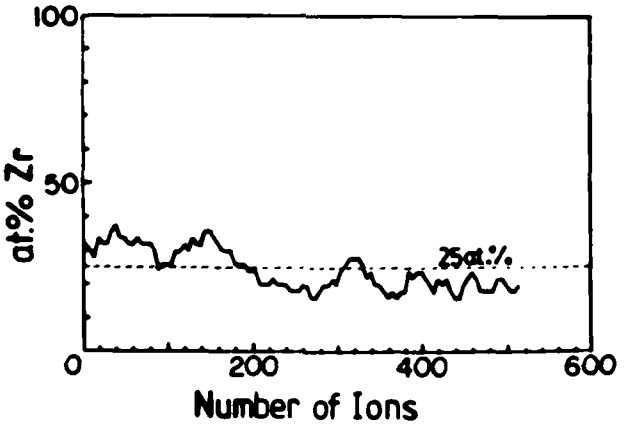

Fig. 6b. Concentration profile of β'.

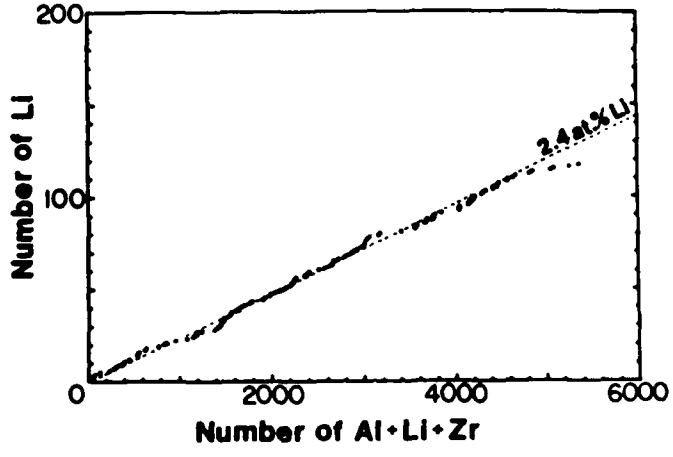

Fig. 6c. Cumulative number of Li atoms detected as a function of total number of Al+Li+Zr.

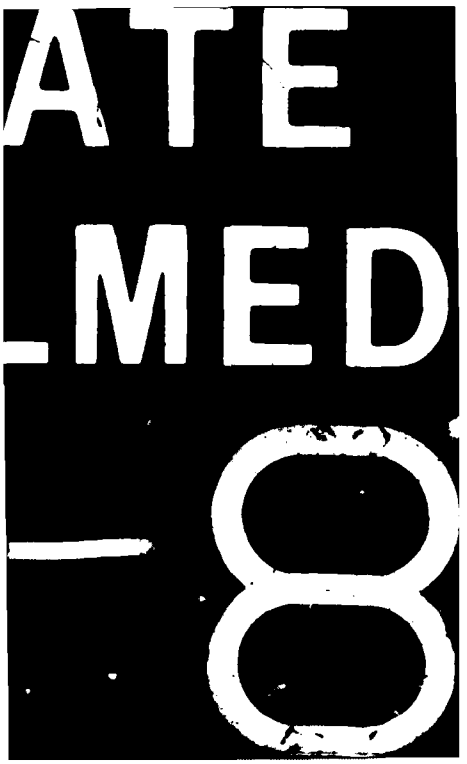
ATE
LMED
8